Two-photon resonant four-wave mixing and multiphoton ionization of cesium in a heat-pipe oven

S. M. Hamadani*
Department of Physics and Astronomy, Western Kentucky University, Bowling Green, Kentucky 42101

J. A. D. Stockdale and R. N. Compton†
Chemical Physics Section, Health and Safety Research Division, Oak Ridge National Laboratory, Oak Ridge, Tennessee 37831

M. S. Pindzola
Physics Department, Auburn University, Auburn, Alabama 36849
(Received 27 March 1986)

Optical pumping of cesium vapor in a heat-pipe oven in which the energy of two near-infrared photons is close to the $6D$ states results in high conversion efficiency (up to 1.7%) of the near-infrared pump light to intense blue, forward-propagating radiation. The blue light corresponds to the $7P$-$6S$ transition. The dependence of conversion efficiency upon focusing conditions, cell length, and pump intensity is presented. Absorption and gain coefficients are measured in a second heat pipe. The results are discussed in terms of optically pumped stimulated emission (OPSE), stimulated electronic Raman scattering (SERS), and subsequent nonlinear four-wave mixing of two pump-laser photons and one SERS or OPSE infrared photon, leading to parametric generation at $\omega=2\omega_L-\omega_{ir}$. Two-photon resonant, three-photon ionization cross sections are also studied experimentally and theoretically for the case of resonant enhancement at the $6D$ levels of cesium. For comparison, similar results for rubidium are also presented for the $5D$ levels.

INTRODUCTION

Optical and spectroscopic studies in alkali metals are frequently performed in "heat-pipe" ovens[1,2] where the atomic density is varied by controlling the temperature of the central region of the pipe. Buffer gas and cooling coils near the optical windows prevent condensation and resultant degradation of optical transmission. With the addition of a biased collector wire, laser-produced ions or electrons can also be collected and displayed, and a very useful apparatus is obtained where optical and spectroscopic as well as photoionization experiments can be performed simultaneously. The system is particularly attractive in the case of alkali-metal vapors where resonant multiphoton ionization (MPI) processes are accompanied by dominant optical phenomena such as optically pumped stimulated emission (OPSE),[3–6] stimulated electronic Raman scattering (SERS),[4,7] parametric mixing processes,[5,8] and hyper-Raman scattering (see Ref. 9 and others cited therein) in which the significant nonlinear susceptibility of the alkali-metal vapor plays an important role.

In this paper we present the results of an experimental study designed to observe MPI and optical emission phenomena simultaneously when cesium atoms are irradiated by two-photon resonant near-infrared dye-laser pulses. In cesium, the presence of the $6P_{3/2,1/2}$ fine-structure doublet at approximately half the energy of the $6D_{5/2}$ and $6D_{3/2}$ levels greatly enhances the transition probability from the $6S_{1/2}$ ground state to the $6D$ states. Similar situations occur in potassium,[3] barium,[10] and sodium.[2,4,11] After excitation to or near the $6D$ level, absorption of a third photon from the laser beam induces ionization to the continuum. Alternatively, the cesium atoms can decay to the lower-lying $7P$ states by OPSE or SERS, causing strong forward emission in the infrared corresponding to the $6D$-$7P$ transitions. Finally, parametric four-wave mixing of two laser photons and one infrared photon generates a visible blue forward-propagating beam at $\lambda=455$–460 nm corresponding to the $7P$-$6S$ transition. Figure 1 shows the relevant partial energy-level diagram

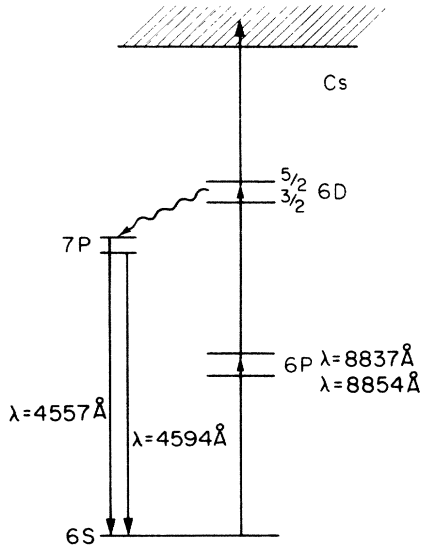

FIG. 1. Partial energy-level diagram of cesium showing the transitions and processes studied in this work.

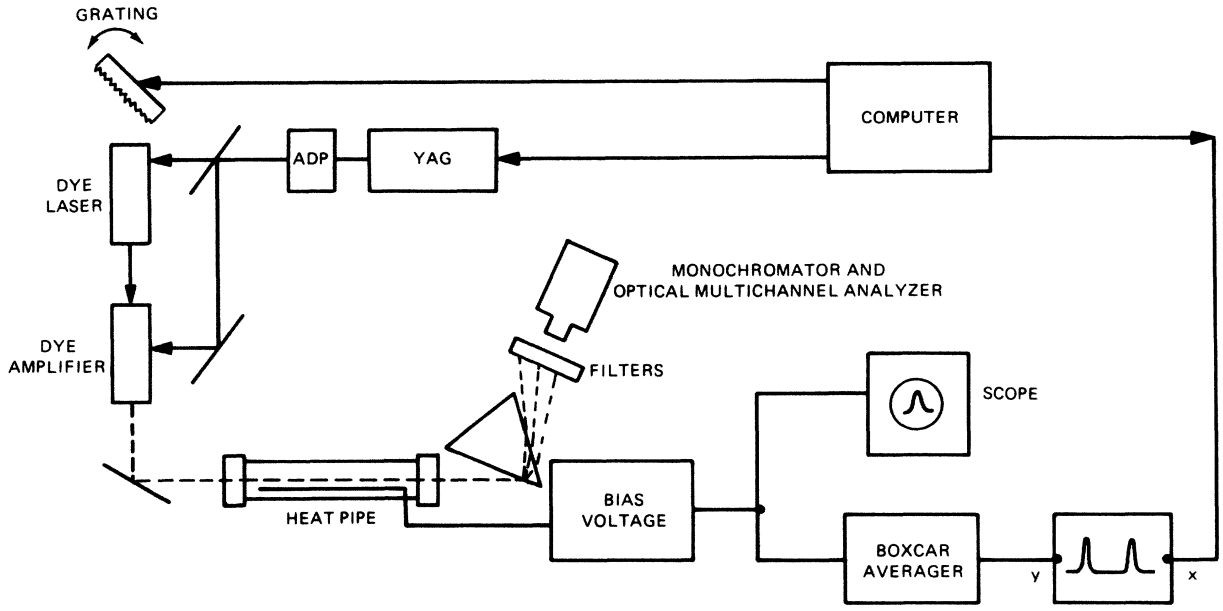

FIG. 2. Experimental arrangement and apparatus. See inset of Fig. 4 for experimental configuration of second heat pipe used in optical gain measurements.

of cesium. The experimental arrangement is shown schematically in Fig. 2.

EXPERIMENT

The output of a frequency-tunable dye laser (Quanta-Ray PDL-1) pumped by the second harmonic ($\lambda=532$ nm) of a Nd:YAG laser (Quanta-Ray DCR-2, YAG is yttrium aluminum garnet) was transmitted through a heat-pipe oven containing saturated cesium vapor at a pressure controlled by the temperature of the pipe ($20 \leq T \leq 400$ °C). In most studies a background buffer-gas (argon or helium) pressure of 3 Torr was used. The dye-laser output could be tuned from 800 to 900 nm with a typical bandwidth of 0.2 Å. The dye-laser output of $\simeq$30 mW average power consisted of 6-ns [full width at half maximum (FWHM)] pulses of power density $\simeq$5 MW/cm^2 for an approximately uniform beam of diameter 3.5 mm at 10 Hz repetition rate. Two different stainless-steel heat pipes were used in these experiments: a 75-cm-long pipe of 2.5 cm inner diameter with an active length of 38 cm between the cooling coils, and a 25-cm-long, 1.5-cm-internal-diameter pipe with a distance of 13 cm between the cooling coils. The central portions of the pipes were resistively heated with ceramic-insulated nichrome wire. The ionization signal, represented as a positive or negative voltage due to the ionic or electronic flow through a 10-kΩ resistor to ground, was displayed on an oscilloscope and averaged by a gated boxcar averager, the output of which was displayed on an X-Y recorder where the X axis corresponded to the frequency of the dye laser and was driven by the dye laser's microprocessor. Light emission in the forward direction was isolated from the pump and analyzed by use of prisms, dielectric filters, polarizer-analyzers, and detected by photodiodes, power meters, or an optical multichannel analyzer (OMA).

Two-photon excitation of the $6d\,^2D_{3/2}$ and $6d\,^2D_{5/2}$ levels in cesium can be achieved by tuning the dye-laser output to $\lambda=885.4$ or 883.7 nm, respectively (see Fig. 1). The laser dye (Exciton) LDS 867 was used in this part of the experiment. This dye has a broad emission capability in the (840—920)-nm region and maximum power at $\lambda_{peak}\simeq870$ nm when pumped by the 532-nm second harmonic of the YAG laser. As mentioned above, the presence of the $6p\,^2P_{1/2}$ and $6p\,^2P_{3/2}$ levels resonantly enhances the two-photon excitation rates and strong ionization signals are observed at resonance. Figure 3 shows the infrared laser power transmitted through (a) the heat pipe, (b) the MPI signals, and (c) the "blue"-light intensity emitted in the forward direction, obtained when the dye-laser wavelength was scanned between 910 and 840 nm. Absorption was observed at the $6p\,^2P_{1/2,3/2}$ and $6d\,^2D_{3/2,5/2}$ resonances. At these high densities absorption at the broader $6P_{3/2}$ and $6P_{1/2}$ one-photon resonances causes subsequent collisional ionization from the excited $6P$ states (energy pooling) according to $Cs^*(6P)+Cs^*(6P)\rightarrow Cs_2^+ + e$. The ionization signals due to these resonances were observed to grow rapidly with temperature. This process was first reported in 1931 (Ref. 12) and has been thoroughly studied[13–16] subsequently. Under high-power laser irradiation, other processes of the type $Cs^* + Cs + h\nu \rightarrow Cs_2^+ + e$ are possible.

As shown in Fig. 3, the two-photon absorption dips at $\lambda=883.7$ and 885.4 nm, leading to the excitation of the $6d\,^2D_{5/2,3/2}$ states, were observed to be much narrower than the $6P$ resonances because of the reduced collisional broadening in this case. Panel (c) of Fig. 3 shows a typi-

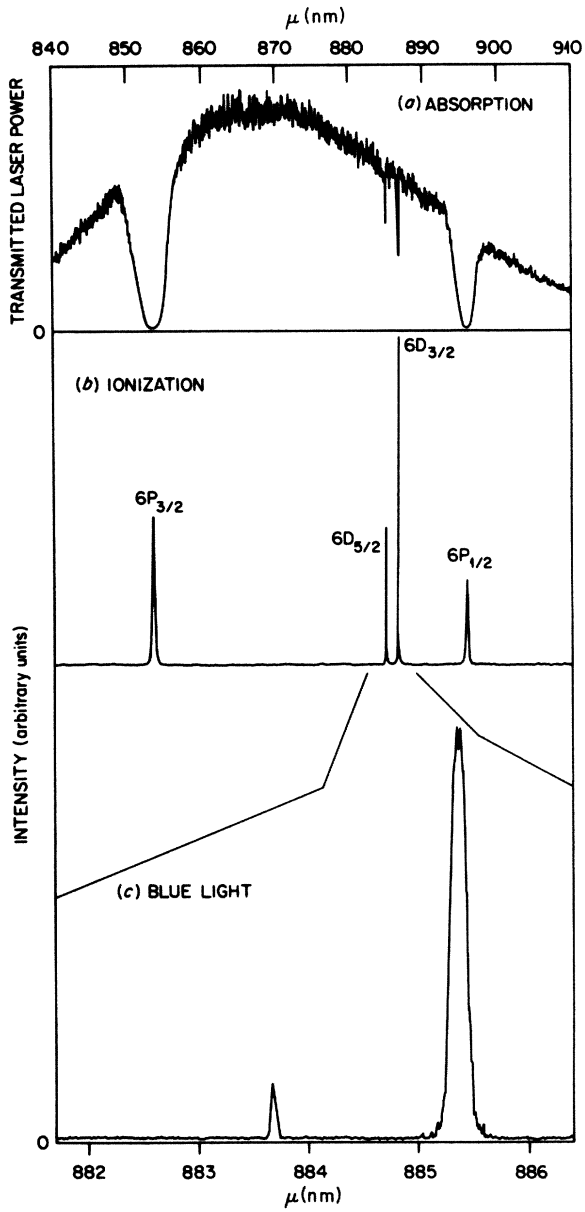

FIG. 3. Wavelength scan of the dye laser between $\lambda=910$ and 840 nm: (a) intensity of transmitted laser light, (b) multiphoton ionization signals, and (c) intensity of blue light in the forward direction.

cal scan of the blue light emitted in the forward direction, collinear with the dye-laser beam. Study of the temporal behavior of this emission indicated that the duration of the pulse was comparable to that of the pump-laser pulse (~ 6 ns), confirming the stimulated character of the radiation. Spectroscopic analysis of the emission using the OMA as well as a grating spectrometer showed that the blue light consisted of $\lambda=455.7$ and 459.4 nm radiation, characteristic of the $7\,^2P_{3/2}-6\,^2S_{1/2}$ and $7\,^2P_{1/2}-6\,^2S_{1/2}$ transitions, respectively. In particular, as seen in Fig. 3, when tuning to the $6d\,^2D_{3/2}$ two-photon resonance, both the ionization signal and the blue-light emission were stronger than when tuning to the $6d\,^2D_{5/2}$ level, in agreement with theoretical considerations to be presented below. Furthermore, the emission occurred only at 455.7 nm in the former case, while both components at 455.7 and 459.4 nm were observed in the latter case. These results are consistent with the selection rules governing the $6D$-$7P$ transitions ($\Delta J=0,\pm 1$).

FOUR-WAVE MIXING RESULTS

The conversion efficiency of the two-step process leading to $7P$-$6S$ blue light was determined by measuring the average powers of the infrared-laser pump beam at the input of the cell, and the power of the blue emission at the output (taking into account the transmission, $T=70\%$, of the dielectric blue filter used to isolate the emission). Table I shows the conversion efficiencies obtained for the two heat pipes of different lengths.

When focusing in the short heat pipe with an $f=15$ cm lens in such a way that the focal waist is located near the position of the cooling coil nearest to the input window, higher conversion efficiencies were obtained. For the case of the $6d\,^2D_{3/2}$ resonant level the efficiency was increased from 0.8% to 1.7%. It is important to note that these conversion efficiencies are about 2 orders of magnitude larger than those reported for similar processes in other alkali-metal vapors,[3–6] except for that reported by Hartig for the case of sodium.[11] When the input beam was focused in the heat pipe, as described above, the tuning range of the laser in which the blue emission was still observed increased from $\sim\pm 0.3$ nm around the $6D_{3/2}$ resonance [see Fig. 3(c)] to $\sim\pm 1$ nm, indicating that a broader range of phase-matching conditions can be satisfied in this case. A corresponding increase was also observed for the $6D_{3/2}$ peak.

The above results are consistent with OPSE on resonance and SERS off resonance, as discussed in more detail below. The blue-light frequency is always coincident with the $7P$-$6S$ transition and clearly results from parametric four-wave mixing of two-laser photons and one OPSE or SERS infrared photon which gives $\omega=2\omega_L-\omega_{ir}$.

The high intensity of the blue emission in the case of cesium is indicative of a very high gain for wavelengths corresponding to the $7P$-$6S$ transition. In order to characterize this gain more accurately, a series of experiments using both heat pipes was performed (see Fig. 4), where the blue emission was generated in the first pipe ($l=38$ cm) and its absorption or gain measured in the second pipe ($l=13$ cm). By inserting an interference filter ($\lambda_{peak}=4500$ Å, $\Delta\lambda=500$ Å, $T\simeq 70\%$) between the two pipes, the blue beam is isolated. In the small signal regime, it then undergoes absorption according to

TABLE I. Unfocused conversion efficiencies in cesium.

Transition	Short pipe $L=13$ cm (%)	Long pipe $L=38$ cm (%)
$6d\,^2D_{3/2}$	0.8	1.0
$6d\,^2D_{5/2}$	0.4	0.5

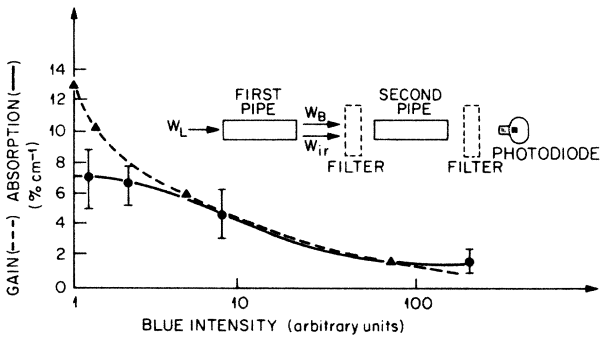

FIG. 4. Gain (upper curve) and absorption coefficient (lower curve) for the blue light created in the first heat pipe ($L=38$ cm), as measured in the second heat pipe ($L=13$ cm). The blue filter is positioned before the second pipe for absorption measurements of α, and after the second pipe for the measurement of gain, g. W_L is the pump-beam intensity, W_{ir} is the infrared OPSE or SERS beam intensity, and W_B is the blue-beam intensity.

$$I_1=I_0e^{-\alpha l}. \tag{1}$$

The intensities I_1 and I_0 are detected by a photodiode and their ratio determines α. Measurements of α at different input intensities I_0 are plotted in Fig. 4. I_0 is varied by placing calibrated neutral density filters at the input of the second pipe. When the interference filter is moved to the output of the second pipe, however, the second pipe is also pumped by that portion of the dye-laser beam not absorbed by the first heat pipe: gain at the $7P$-$6S$ transition will therefore appear, leading, in the small regime, to a signal of magnitude

$$I_2=I_0e^{gl}. \tag{2}$$

The ratio $I_2/I_1=\exp[(g+\alpha)l]$ therefore allows us to measure g after subtraction for the value of α as obtained in the first part of the experiment at the same input intensity. Moving the blue filter from the input to the output side of the short pipe allows the determination of I_2/I_1 on the same detector. It must be noted, however, that the value of gain obtained by this method is strongly intensity dependent and particular care must be taken to allow for the effects of the infrared-pump laser-beam intensity. As can be seen in Fig. 4, the absorption coefficient α is also intensity dependent and its value is reduced from the small-signal value of 0.07 cm^{-1} to 0.02 cm^{-1} when the input intensity is increased by 2 orders of magnitude. This reduction is not due only to saturation of the absorption at the high-power densities. The intensities used are much too weak to saturate the transition. It occurs primarily because of self-absorption in the first heat pipe. Radiation emitted near the entrance window is resonant with the $6S\rightarrow 7P$ transitions and is absorbed by the remaining layers. Due to axial pressure gradients along the pipe, the central portion of the spectrum is more strongly attenuated than the wings, leading to a "self-reversed" spectrum which is depleted at resonance, and consequently yields lower absorption in the second heat pipe. This effect is probably the dominant cause of the decrease in α at higher intensities. The gain coefficient g is expected to increase quadratically with the pump-beam intensity, since for both OPSE and SERS g is proportional to I_{ir}^2 (see Refs. 5, 10, and 17). In order to characterize the gain, the infrared intensity I_{ir} transmitted through the neutral density filters and entering the second pipe was also measured. The g values obtained above were then renormalized by multiplying by $(I_{ir}^{max}/I_{ir})^2$. I_{ir}^{max} is the maximum infrared power used (corresponding to the highest gain point, average power 4.5 mW). The upper curve of Fig. 4 is thus obtained, which shows the results of the measurement of the gain coefficient when the infrared pump beam of average power 4.5 mW is resonant with the $6D_{3/2}$ two-photon transition and the intensity of the probe blue light is varied. A maximum value of $g=0.13$ cm^{-1} is obtained in the small-signal regime.

The experimental results described above are in agreement with theoretical considerations based on the theory of four-wave mixing processes[5,10,17,18] in which the induced polarization at $\omega_{blue}=2\omega_L-\omega_{ir}$ is given by

$$P_B=\epsilon_0\chi^{(3)}(\omega_B)E_L^2E_{ir}^*, \tag{3}$$

where E_L and E_{ir} are the electric fields of the laser wave and the laser-induced infrared wave, respectively, and $\chi^{(3)}(\omega_B)$ designates the third-order susceptibility of the process:

$$\chi^{(3)}(\omega_B)=\frac{KN}{\hbar^3}\sum_{i,j,k}\frac{\mu_{gi}\mu_{ij}\mu_{jk}\mu_{kg}}{(\Omega_i-\omega_L)(\Omega_j-2\omega_L)(\Omega_k-\omega_B)}, \tag{4}$$

with N the atomic number density, μ_{ij} the dipole matrix element for the transition $i\rightarrow j$, and $\Omega_i=(E_i-E_g)/\hbar-i\Gamma_i$; K is a numerical factor depending on the number of distinguishable frequencies.[19] Neglecting the depletion of the laser wave, and the reabsorption of the blue wave and assuming an exponential increase of the infrared wave $E_{ir}(z)=E_{ir}^0\exp(g_{ir}z/2)$ along the medium, the emitted light intensity can be calculated by solving the wave equation to give

$$I_B(Z)=\frac{\epsilon_0^2\eta_B\eta_L^2\eta_{ir}\omega_B^2\,|\chi_B^{(3)}|^2I_L^2I_{ir}(z)}{g_{ir}^2+4(\Delta k)^2}, \tag{5}$$

where $\eta=(\mu_0/\epsilon_0\epsilon)^{1/2}$, $\Delta k=2k_L-k_{ir}-k_B$ is the collinear phase mismatch, and g_{ir} is the gain of the infrared wave. In particular, we see that, if the pump power is large enough so that $g_{ir}^2\gg 4(\Delta k)^2$, the phase-matching condition $\Delta k=0$ is not significantly important. If $g_{ir}^2\leq 4(\Delta k)^2$, on the other hand, nonlinear phase matching can be achieved by using the divergence of the laser or by focusing the beams in the cell.

In the present experiment the third-order susceptibility $\chi^{(3)}(\omega_B)$ is resonantly enhanced by the following factors: (a) the presence of the $6P$ levels at $\Omega_{6P\text{-}6S}\simeq\omega_L$ enhance the one-photon term $(\Omega_i-\omega_L\simeq 0)$, (b) the $6D_{3/2,5/2}$ levels at $\Omega_{6D\text{-}6S}\simeq 2\omega_L$ resonantly enhance the two-photon term $(\Omega_j-2\omega_L=0)$, and (c) the $7P_{1/2,3/2}$ levels are resonant with the emitted blue light, such that also the last term in the denominator, $\Omega_K-\omega_B=\Omega_{7P\text{-}6S}-\omega_B=0$, vanishes. The above resonant denominators are in this case replaced by terms including the width of the appropriate transition, Γ_i, thus preventing $\chi^{(3)}(\omega_B)$ from diverging.[17,20] The nonlinear susceptibility is triply enhanced by the above simultaneous resonances, which, in turn, results in the

high intensity of the blue-light generation, as given by Eq. (5).

IONIZATION RESULTS

Three-photon ionization cross sections resonantly enhanced by the $6D_{3/2}$ and $6D_{5/2}$ states were determined from measurements of the laser fluence, laser space and time profile, absolute ion yields, and cesium-atom density. The laser beam was unfocused. These measurements were performed at room temperature, where the number density was low enough to assume that no collisional ionization processes are operative, space-charge effects are minimal, and stimulated emission processes such as those discussed in the preceding section will not complicate the analysis. The cesium number density was determined by measuring the ion yields in the room-temperature heat pipe using the output of the fourth harmonic of the Nd:YAG laser (266 nm). Using the known photoionization cross section at 266 nm,[21] we determined a cesium-atom number density of 3×10^{11} cm^{-3} at $T=300$ K. The dye-laser beam profile was determined using a photodiode behind a movable slit of width 0.5 mm. The beam diameter was 3.5 mm FWHM. The laser power was determined with a calibrated Scientech calorimetric power meter. The number of ions produced per laser shot, N_i, was determined by photographing the voltage pulse across a 10^4-Ω resistor and performing the integral

$$N_i=\frac{1}{e}\int_0^\infty V(t)\frac{dt}{R}, \tag{6}$$

where $e=1.6\times10^{-19}$ C/electron, $R=10^4$ Ω, and $V(t)$ is the measured time dependence of the voltage pulse. Typical values for N_i were 10^8–10^{10} ions/pulse. Measurements were made only in the region where the ion yield varies as the cube of the laser power.

An effective three-photon ionization cross section is given by

$$\hat{\sigma}=\frac{N_i}{g^{(3)}\{n\}V\tau}I^3, \tag{7}$$

where $g^{(3)}$ is the third-order normalized correlation function. Debethune[22] has shown that, in the limit of an infinite number of independent modes of the laser, $g^{(m)}$ can be approximated by $m!$. Thus, we take $g^{(3)}$ to be 6. In Eq. (7), $\{n\}$ is the cesium-atom number density, V and τ are the third-order interaction volume and time, respectively, and I is the laser fluence (number of photons cm^{-2}s^{-1}). Using Eq. (7) we determine *apparent* values of $\hat{\sigma}$ to be 10^{-69} cm^{6}s^2 for the $6D_{3/2}$ state and 2.5×10^{-70} cm^{6}s^2 for the $6D_{5/2}$ state. These cross sections are determined for the case in which the laser is tuned to resonance (i.e., maximum signal). Since the homogeneous linewidth of the resonance at these laser powers is much narrower than the bandwidth of the laser, these cross sections are a lower limit to the true cross section at the resonance position. An approximate value for the resonant cross section can be obtained from knowledge of the laser bandwidth ($\Gamma\simeq0.2$ Å), and the natural width of the resonance ($\Delta\lambda_n$). For a two-photon resonant three-photon ionization process, a first-order correction to the resonant cross section can be obtained by multiplying the measured cross section by the square of the ratio of the laser bandwidth to the natural width of the level. For two-photon excitation of the $6D$ levels this factor is $(0.2/0.0001)^2$, or $\sim4\times10^6$. This gives approximate resonant cross sections of $\hat{\sigma}_{3/2}\simeq4\times10^{-63}$ cm^{6}s^2 and $\hat{\sigma}_{5/2}\simeq10^{-63}$ cm^{6}s^2. Due to the approximation involved, these cross sections are expected to be accurate to only 1 or 2 orders of magnitude. The ratio $\hat{\sigma}_{3/2}/\hat{\sigma}_{5/2}=4$ is, of course, more accurate and provides a better test of theory. As a further test of this procedure, similar measurements were performed for the case of two-photon resonant three-photon ionization of rubidium in which the laser is tuned to two-photon resonance with the $5d\,^2D_{5/2}$ and $5d\,^2D_{3/2}$ states. In this case the directly measured three-photon ionization cross sections are $\hat{\sigma}_{5/2}=10^{-67}$ cm^{6}s^2 and $\hat{\sigma}_{3/2}=6\times10^{-69}$ cm^{6}s^2. The natural width of the $D_{5/2}$ or $D_{3/2}$ level in terms of the two-photon laser wavelength is $\Delta\lambda_n=0.000\,02$; therefore the measured cross sections can be multiplied by $(0.2/0.000\,02)^2$, or 10^8, to obtain an approximate resonance cross section. This results in $\hat{\sigma}_{5/2}=10^{-59}$ cm^{6}s^2 and $\hat{\sigma}_{3/2}=6\times10^{-61}$ cm^{6}s^2. For rubidium, ionization via the $J=\frac{5}{2}$ state is ~17 times greater than the $J=\frac{3}{2}$ state. By contrast, note that for cesium $\hat{\sigma}_{3/2}$ is *larger* than $\hat{\sigma}_{5/2}$ by a factor of 4. As we will see below, the near resonance of the $6P$ and $5P$ states at the one-photon level for cesium and rubidium, respectively, play an important role in the multiphoton ionization process.

The experimental results described above may be treated using a stochastically averaged density-matrix formalism based on an ideal chaotic radiation field.[23] At low densities, however, the effective three-photon ionization cross section defined by Eq. (7) is simply proportional to the square of the flux-independent part of the two-photon Rabi rate, $R_{\alpha\beta}$, given by[24]

$$R_{\alpha\beta}=\frac{4\pi\omega}{c}\sum_n\frac{\mu_{\beta n}\mu_{n\alpha}}{E_\alpha-E_n+\hbar\omega}. \tag{8}$$

Since the fine-structure levels for cesium and rubidium are observed in the experiment, the dipole matrix elements in Eq. (8) are reduced to radial form using *lsj*-coupled single-configuration wave functions. The sum over intermediate states found in Eq. (8) is determined by the inhomogeneous-differential-equation technique.[24] For cesium $|R(6S_{1/2}\rightarrow6D_{3/2})|=8.3\times10^{-16}$ cm^2 and $|R(6S_{1/2}\rightarrow6D_{5/2})|=3.5\times10^{-16}$ cm^2, while for rubidium $|R(5S_{1/2}\rightarrow5D_{3/2})|=3.6\times10^{-17}$ cm^2 and $|R(5S_{1/2}\rightarrow5D_{5/2})|=6.3\times10^{-16}$ cm^2. The two-photon Rabi rates for both cesium and rubidium are strongly influenced by the near resonance with the $6P$ and $5P$ levels, respectively. Since the excited-state photoionization cross sections for both D levels of either cesium or rubidium are approximately the same,[24] the fine-structure ratio of the experimental effective cross sections defined by Eq. (7) is given by

$$\frac{\hat{\sigma}_{3/2}}{\hat{\sigma}_{5/2}}=\left[\frac{R(nS_{1/2}\rightarrow nD_{3/2})}{R(nS_{1/2}\rightarrow nD_{5/2})}\right]^2. \tag{9}$$

For cesium, theory predicts $\hat{\sigma}_{3/2}/\hat{\sigma}_{5/2}=5.6$, while for rubidium $\hat{\sigma}_{5/2}/\hat{\sigma}_{3/2}=17.6$. Both results are in good agreement with the experimental values given in the previous paragraph.

Finally, we should emphasize that these measurements on MPI cross sections were performed at low atom densities where competing effects, e.g., hyper-Raman effects, collisional ionization, or relaxation, etc., are negligible. In addition, Malcuit, Gauthier, and Boyd[25] have recently observed suppression of amplified spontaneous emission (ASE) by four-wave mixing in sodium vapor. They studied two-photon resonant excitation of the sodium $3d$ level leading to new frequencies either by ASE at the $3d \rightarrow 3p$ frequency or by resonantly enhanced four-wave mixing. Competition between the two pathways was observed. Such phenomena may also influence the ionization rate at high densities and high laser power. Experiments designed to study such effects upon MPI would also be of interest, but would be more difficult to perform due to space-charge suppression of ion collection.

CONCLUSIONS

Two-photon resonant four-wave mixing in cesium at the $6D$ resonant states results in high conversion efficiencies (up to 1.7%) for the near-infrared light into intense blue, forward-propagating radiation. Two-photon resonant three-photon ionization cross sections via the $6D_{3/2,5/2}$ and intermediate states of cesium and the $5D_{3/2,5/2}$ states of rubidium have been determined experimentally. The ratios of the results for the fine-structure states are in good agreement with theoretical estimates. The near resonance at the energy level of the first photon plays an important role in both the wave mixing and multiphoton ionization processes.

ACKNOWLEDGMENT

This research was sponsored by the Office of Health and Environment Research, U.S. Department of Energy, under Contract No. DE-AC05-84OR21400 with Martin Marietta Energy Systems, Inc., and in part by the Oak Ridge Associated Universities.

---

*Present address: Laseronics, Inc., 6399 Wilshire Boulevard, Los Angeles, CA 90048.

†Also at Department of Chemistry, The University of Tennessee, Knoxville, TN 37996.

[1]C. R. Vidal and J. Cooper, J. Appl. Phys. **40**, 3370 (1969).

[2]D. Cotter and D. C. Hanna, Opt. Quantum Electron. **9**, 509 (1977).

[3]P. Agostini, P. Bensousan, and J. Coulassier, Opt. Commun. **5**, 293 (1972).

[4]D. Cotter, D. C. Hanna, W. H. W. Tuttlebee, and M. A. Yuratich, Opt. Commun. **22**, 190 (1977).

[5]P. L. Zhang, Y. C. Wang, and A. L. Schawlow, J. Opt. Soc. Am. **1**, 9 (1984).

[6]S. A. Bakhramov, U. G. Gulyamov, K. N. Drabovich, and Y. A. Z. Faizullaev, Pis'ma Zh. Eksp. Teor. Fiz. **21**, 229 (1975) [JETP Lett. **21**, 102 (1975)].

[7]F. A. Korolev, S. A. Bakhramov, and V. I. Odintsov, Pis'ma Zh. Eksp. Teor. Fiz. **12**, 131 (1970) [JETP Lett. **12**, 90 (1970)].

[8]F. A. Korolev, S. A. Bakhramov, and V. I. Odintsov, Opt. Spektrosk. **30**, 788 (1971) [Opt. Spectrosc. (USSR) **30**, 425 (1971)].

[9]Yu. P. Malakyan, Kvant. Elektron. (Moscow) **12**, 1365 (1985) [Sov J. Quantum Electron. **15**, 905 (1985)].

[10]J. Heinrich and W. Behmenburg, Appl. Phys. **23**, 333 (1980).

[11]W. Hartig, Appl. Phys. **15**, 427 (1978).

[12]K. Freudenberg, Z. Phys. **67**, 417 (1931).

[13]A. Klyucharev, V. Sepman, and V. Vujnovic, J. Phys. B **10**, 715 (1977).

[14]A. G. F. Kniazzeh, Bull. Am. Phys. Soc. **11**, 634 (1966).

[15]A. N. Klyucharev and N. S. Rgazanov, Opt. Spektrosk. **33**, 425 (1972) [Opt. Spectrosc. (USSR) **33**, 230 (1972)].

[16]B. V. Dobrolezh, A. N. Klyucharev, and V. Yu Sepman, Opt. Spektrosk. **38**, 1090 (1975) [Opt. Spectrosc. (USSR) **38**, 630 (1975)].

[17]D. C. Hanna, M. A. Yuratich, and D. Cotter, in *Nonlinear Optics of Free Atoms and Molecules*, Vol. 17 of *Springer Series in Optical Sciences* (Springer-Verlag, Berlin, 1979).

[18]A. Corney and K. Gardner, J. Phys. B **12**, 1425 (1979).

[19]B. J. Orr and J. F. Ward, Mol. Phys. **20**, 513 (1971).

[20]John F. Reintjes, in *Nonlinear Optical Parametric Processes in Liquids and Gases* (Academic, New York, 1984).

[21]H. Suemitsu and J. A. R. Samson, Phys. Rev. A **28**, 2752 (1983).

[22]J. L. Debethune, Il Nuovo Cimento **12**, 101 (1972).

[23]P. Agostini, A. T. Georges, S. E. Wheatley, P. Lambropoulos, and M. D. Levenson, J. Phys. B **11**, 1733 (1978).

[24]M. S. Pindzola, A. H. Glasser, and M. G. Payne, Phys. Rev. A **30**, 1800 (1984).

[25]M. S. Malcuit, D. J. Gauthier, and R. W. Boyd, Phys. Rev. Lett. **55**, 1086 (1985).